Pseudo-direct bandgap transitions in silicon nanocrystals: effect on optoelectronics and thermoelectrics

Vivek Singh,[1] Yixuan Yu,[2] Qi-C. Sun,[1] Brian Korgel,[2] Prashant Nagpal[1,3,4*]

[1]Department of Chemical and Biological Engineering, University of Colorado Boulder

[2]Mc Ketta Department of Chemical Engineering, Texas Materials Institute, and Center for Nano- and Molecular Science and Technology, University of Texas at Austin

[3]Materials Science and Engineering, University of Colorado Boulder

[4]Renewable and Sustainable Energy Institute (RASEI), University of Colorado Boulder

Corresponding Author:* Email: pnagpal@colorado.edu

Supporting Information

Methods

Synthesis of Silicon Nanocrystals [21,S1-S3]:

Materials: FOx-16 (16% hydrogen silsesquioxane (HSQ) by weight in methyl isobutylketone) purchased from Dow-Corning, ethanol, toluene, hexanes, chloroform, and hydrochloric acid (HCl, 37.5%) were purchased from Fisher Scientific, hydrofluoric acid (HF, 48%) was purchased from EMD chemicals and deionized (DI) water was obtained using a Barnstead Nanopure Filtration System (17 MΩ resistance).

Synthesis: 4g of HSQ was heated under forming gas (7% hydrogen gas and 93% nitrogen gas) flow at temperatures ranging from 1100-1300^{o}C for 1 hour. Nanocrystals with larger size are obtained from higher temperature decomposition of HSQ. The oxide-embedded Si nanocrystal product was ground with agate mortar and pestle for 10 min and then placed in a wrist-action shaker for 10 hrs in the presence of borosilicate glass beads. The material was etched for 4-6 hrs in the dark by adding 300 mg of ground powder to 1mL of 37% HCl and 10 mL of 48% HF. Si nanocrystals were isolated then by centrifugation at 8000 rpm for 5 min. The Si nanocrystal residue rinsed once with DI water, twice with ethanol, and once with chloroform. The Si

nanocrystals were dispersed with 6 mL of 1-dodecene, degassed with three freeze-pump-thaw, and passivated at 190^{o}C in nitrogen gas flow for 16 hours. Passivated Si nanocrystals could be dispersed in nonpolar solvents like toluene, chloroform, or hexanes. The average nanocrystal sizes of 2.4, 5.6 and 8.3 nm were determined by TEM.

Characterization Setup and Procedure

Low Temperature Photoluminescence and Absorbance measurements:

Setup: The photoluminescence (PL) and absorbance measurements were performed with a low temperature setup with a closed cycle helium cryostat purchased from Advanced Research systems Inc., with the cold head capable of measuring temperature range from 8 K to 300 K. The temperature was controlled by a heating coil assembly connected to a 335 temperature controller purchased from Lake Shore Cryotronics, Inc. The PL and absorbance spectra was obtained by using USB4000 VIS-NIR spectrometer purchased from Ocean Optics, coupled with two optical fiber type VIS-NIR with fiber core diameter of 400 μm.

Procedure: The sample preparation was done by dissolving a mixture of polystyrene pellets in chloroform, using sonication. After the pellets were dissolved, the Si NP dispersion was added. The Si NCs were dispersed in polystyrene film to prevent any energy transfer or electronic coupling between them. This also reduces back scattering, and the refractive index contrast between Si NC film and air. A film from this dispersion was drop-casted on a glass slide and dried in the fume hood for the chloroform to evaporate. The sample was then loaded on the cold-head with a DT-670 diode sensor. For the PL measurements, the sample was excited with incident light (365 nm) and the PL spectra was recorded under different temperatures.

After photoexcitation with higher energy photons (3.1 eV), the photoexcited electrons relax to lower energy states and statistically occupy/sample all possible sates at the bottom of the conduction band. Following this event, the recombination between photoexcited electrons and holes occur, and all optically allowed states are seen using radiative recombination and their energetic positions are revealed by steady state photoluminescence (PL) measured here. The broad energy range of the emitted photons here, measured by the PL FWHM, is compared with the band width of electronic DOS measured from scanning tunneling spectroscopy (STS)

measurements. While the PL width is always larger, it can be explained by partially filling the valence band states with the laser power (~300 mW) used in these experiments

Scanning Tunneling Microscopy and Spectroscopy

Setup: The instrumentation setup consisted of a modified PicoScan 2500 setup (with PicoSPM II controller), an STM nosecone (N9533A series, Agilent Technologies) was used for microscopy and spectroscopy using chemically etched Pt-Ir tips (80:20) purchased from Agilent Technologies, USA.

Procedure: Tunneling junction parameters were set at tunneling current for 0.2 nA for the 2.4 nm Si nanoparticles and sample bias of 0.1 V, 5.6 and 8.3 nm Si nanocrystals at 0.1 nA and sample bias at 0.1 V. All samples were prepared by drop casting dilute solutions on a cleaned indium tin oxide (ITO) coated glass substrate. Spectroscopy measurements were obtained on a scan range from -5 V to + 5V with scan rate of 1V/s. The energy states (or electronic DOS) are measured with respect to the constant work function of the Pt/Ir tip.

Current Sensing Atomic Force Microscopy (CSAFM)

Setup: The instrumentation setup consisted of PicoScan 2500 setup (with PicoSPM II controller), an CSAFM nosecone (N9533A series, Agilent Technologies) was used for CSAFM and spectroscopy. The CSAFM tips used were coated in-house using thermal evaporator with 5 nm of 99.99% Cr and 25 nm of 99.99% Au, both purchased from Kurt J. Lesker Company. The silicon tips for contact mode imaging and spectroscopy were obtained from NanoDevices, Inc. An externally attached monochromator (Model: SP2150i, Princeton Instruments) was connected via an optical cable to direct light below the sample stage. In addition, 2 filters obtained from Thorlabs (BandPass color filter 50.8 mm SQ 315-710 nm and 50.8 mm SQ 715 nm LongPass color filter) were also used at the output of the monochromator. Power obtained for different wavelengths was measured using calibrated power meter (Model: 1918-R) and detector (Model: 818-UV) purchased from Newport.

Procedure: The mode selected for CSAFM measurements was contact mode and the deflection set points were varied between -1 V to -3 V to obtain a current image. The bias voltage was set at

+200 mV. The sample was prepared by drop casting dilute suspensions on cleaned ITO coated substrate. The sample stage was modified by creating a transparent light path for illuminating the samples from underneath the sample stage. The sample placed on a transparent ITO substrate was connected using a wire attached to the ITO using conductive silver paste. The spectroscopy measurements were performed by scanning the applied voltage from -400 mV to +400 mV at a rate of 1 V/s. The sample was excited at different wavelengths from the output of the monochromator. The photocurrent was obtained by taking the difference between the dark current and the current obtained by illumination under different wavelengths.

Thermoelectric Measurements

The thermoelectric measurements were done using the CSAFM setup described earlier, with a sample stage containing a 100 Ω Plat/500 diode sensor capable of temperature ranges between ambient and 250^{o}C. The 335 temperature controller (purchased from Lake Shore Cryotronics, Inc) was PID (proportional, integral and derivative) parameters and the temperature ramp rate for measurements was set to 10^{o}C/min. The measurements were carried out maintaining the gold coated cantilever at room temperature. After the temperature of the stage was stabilized, the spectroscopy measurement was performed with the tip bias voltage measurements ranging from -100 mV to +50 mV, for which the current was recorded.

Measurement of gold tip plasmon resonance

The gold tip plasmon resonance (extinction spectra) was obtained by using home-built confocal setup, using an Axio Observer MAT Inverted Microscope, purchased from Zeiss. Briefly, using a high N.A. (0.8) 100X objective lens, an image of the gold tip was projected through three confocal pinholes and apertures, onto a 400 micrometer fiber optic cable attached at the output port of the microscope. The confocal setup was configured so only the optical spectrum of the gold tip was measured (no interfering effects). The collected light spectrum was analyzed using a spectrophotometer (Ocean optics USB 4000). The spectrum of the light source and a silver reflector were used to calibrate the setup and measure source spectrum for comparison.

The origin of this double peak is the shape of the gold coated AFM tip. The two peaks for plasmon resonances (Figure 4b) represent two different plasmon modes: one higher energy

plasmon closer to the bandedge of Si NC, resonant at ~2 eV (red curve) with Si NC; and a lower energy plasmon mode resonant at ~1.5 eV with Si NC environment. The surface plasmon resonances of these two different modes in air were ~2.23 and 1.87eV (black curve), and were red-shifted on contact with the silicon NC due to the change in the dielectric constant of the effective medium during the photocurrent measurements (red curve). Different AFM tips and gold coatings can yield slightly different plasmon modes, depending on the shape of the tip. This particular gold-coated tip and Si NCs were chosen due to their well-matched bandedge absorption and plasmon resonance modes.

Attenuated total reflectance Fourier transform infrared (ATR-FTIR)

Attenuated total reflectance Fourier transform infrared (ATR-FTIR) spectra were obtained on a Thermo Mattson Infinity Gold FTIR spectrometer equipped with a Spectra-Tech Thermal ARK attenuated total reflectance module. A background measurement was taken after purging with N_2 for 30 min before loading the sample into the ARK attenuated total reflectance module. Nanocrystals dispersed in a solvent (i.e., ethanol, toluene) with concentration of 1 mg/mL were drop-cast onto the crystal plate of the ARK module and dried with N_2. Measurements were made by acquiring 128 scans at a resolution of 4 cm^{-1}. The average transmittance is reported with background subtraction.

X-ray photoelectron spectroscopy (XPS)

X-ray photoelectron spectroscopy (XPS) was performed using a commercial X-ray photoelectron spectrometer (Kratos Axis Ultra), utilizing a monochromatic Al K_α X-ray source ($h\nu$ = 1486.5 eV), hybrid optics (employing a magnetic and electrostatic lens simultaneously), and a multichannel plate detector coupled to a hemispherical analyzer. Si nanocrystal films were drop-cast onto indium tin oxide coated glass slides and were secured on the experimental tray using double-sided Cu tape. The photoelectron takeoff angle was normal to the surface of the sample and 45° with respect to the X-ray beam. All spectra were recorded using a single sweep and an aperture slot of 300 μm by 700 μm. High-resolution spectra were collected with 20 eV pass energy. Spectra were collected at 0.1 eV intervals and 1500 ms integration time through a

tungsten coil set at 4.8 V bias with respect to the sample. The pressure in the analysis chamber was typically 3×10^{-9} Torr during data acquisition. Sample charging was corrected by shifting the Si^0 $2p_{3/2}$ to a binding energy of 99.3 eV. Background subtraction was done using a Shirley background model. The Si^0 $2p_{3/2}$ and Si^0 $2p_{1/2}$ peaks were fit with Voigt profiles (30% Gaussian character) centered at 99.3 and 99.8 eV, respectively, maintaining the appropriate intensity ratio of 2:1corresponding to the spin−orbit splitting ratio for p-orbitals. Peak contributions from Si^{1+}, Si^{2+}, Si^{3+}, Si^{4+}, and Si−C were fit using Voigt profiles centered at 100.4, 101.5, 102.6, and 103.7, and 102.0 eV, respectively.

Supporting Information

FIGURES

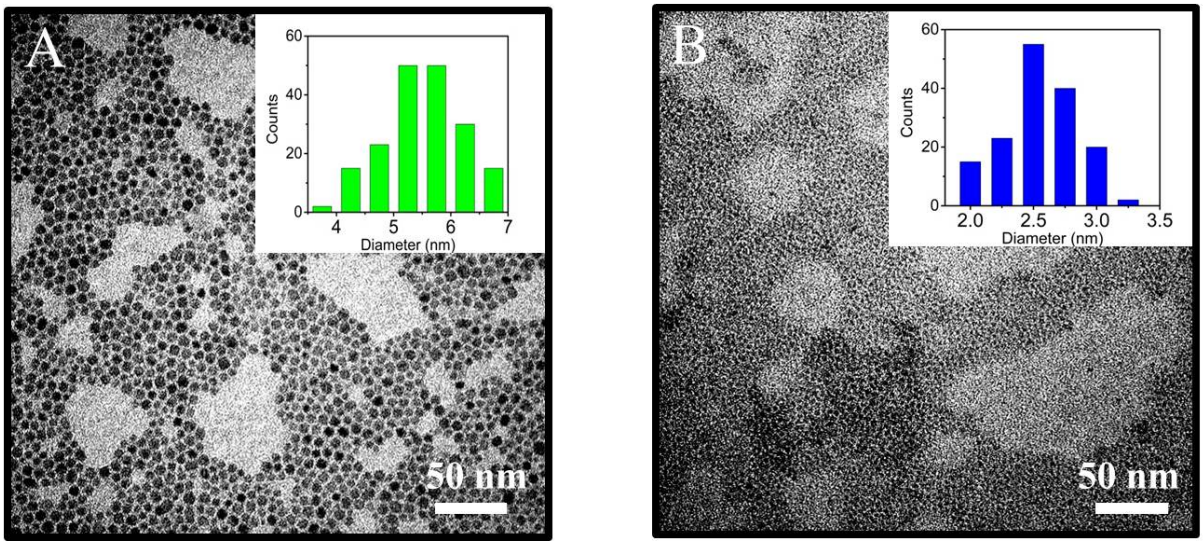

Figure S1: TEM images of the 1-dodecene passivated Si nanocrystals with average diameters of (A) 5.6 nm s and (B) the 2.4 nm. The histrograms of nanocrystal diameter determined from each image are provided in the insets.

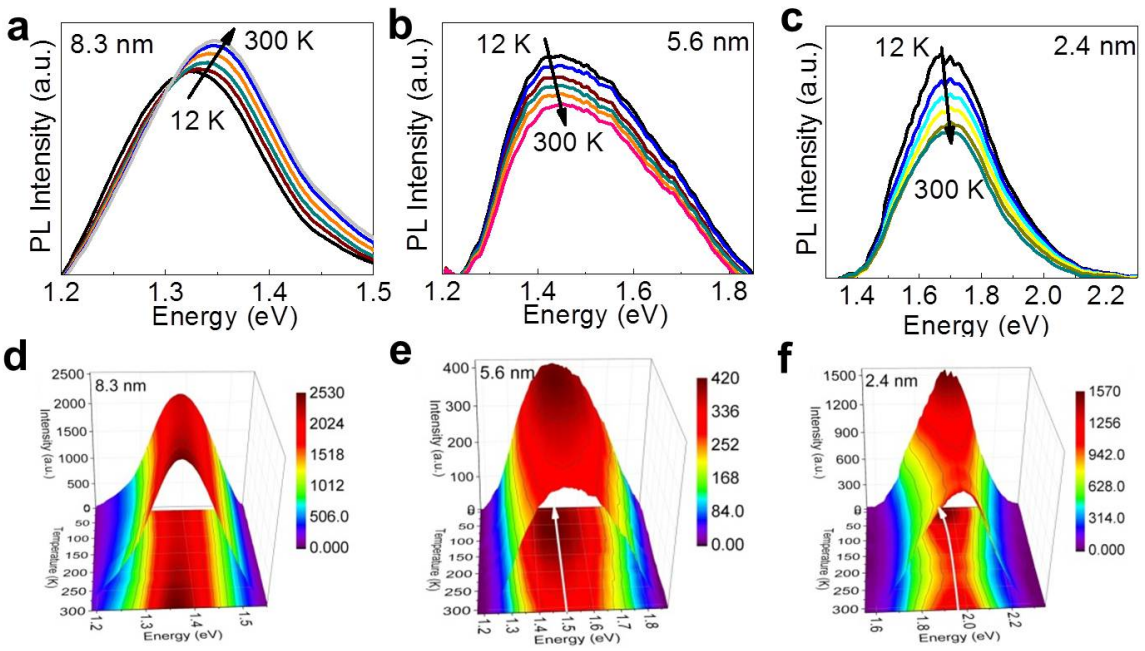

Figure S2. Size-dependent photophysics in silicon nanocrystals. (a) Two-dimensional (2D) plot for PL with temperature for 8.3 nm Si NC, showing a decrease in PL intensity with decrease in temperature. 2D PL plot, for (b) 5.6 nm Si NCs; and (c) 2.4 nm Si NCs, show increase in PL with decrease in temperature. (d) 3D plots of PL with temperature for 8.3 nm Si NC, showing a decrease in PL intensity with decrease in temperature. 3D PL plot, for (e) 5.6 nm Si NCs; and (f) 2.4 nm Si NCs, showing increase in PL with decrease in temperature,

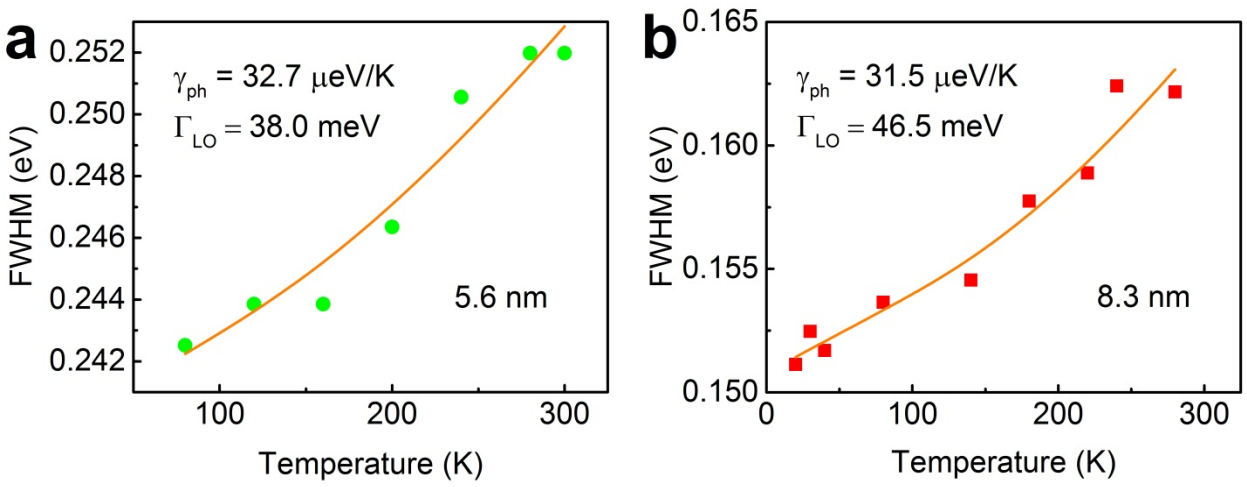

Figure S3 FWHM of PL as a function of temperature for (a) 5.6 nm, and (b) 8.3 nm Si NCs, respectively. The orange lines show the fitting results using Equation 1.

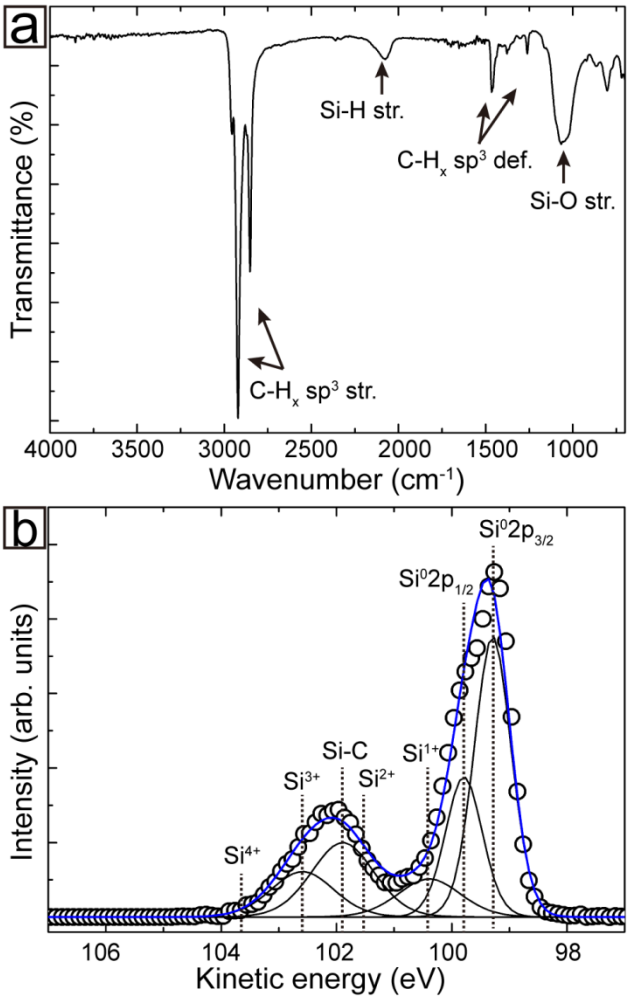

Figure S4. (a,b) ATR-FTIR and XPS for silicon NCs, characterizing the ligands and NC surface.

References

(S1) C. M. Hessel, D. Reid, M. G. Panthani, M. R. Rasch, B. G. Goodfellow, J. Wei, F. Hiromasa, V. Akhavan, and B. A. Korgel, *Chem. Mater.*, 2012, **24**, 393-401.

(S2) C. M. Hessel, J. Wei, D. Reid, F. Hiromasa, M. C. Downer and B. A. Korgel, *J. Phys. Chem. Lett.*, 2012, **3**, 1089-1093.

(S3) M. G. Panthani, C. M. Hessel, D. Reid, G. Casillas, M. J. Yacaman and B. A. Korgel, *J. Phys. Chem. C*, 2012, **116**, 22463-22468.

(S4) Y. Yixuan M. Colin, Hessel, T. D. Bogart, M. G. Panthani, M. R. Rasch and B. A. Korgel, *Langmuir*, 2013, **29**, 1533-1540.